Investigation of CeO2 Buffer Layer Effects on the Voltage Response of YBCO Transition-Edge Bolometers

Mohajeri, Roya; Nazifi, Rana; Wulff, Anders Christian; Vesaghi, Mohammad A.; Grivel, Jean-Claude; Fardmanesh, Mehdi

Published in:
I E E E Transactions on Applied Superconductivity

Link to article, DOI:
10.1109/TASC.2016.2535144
10.1109/TASC.2016.2535144

Publication date:
2016

Document Version
Peer reviewed version

Investigation of CeO_2 Buffer Layer Effects on the Voltage Response of YBCO Transition Edge Bolometers

Roya Mohajeri, Rana Nazifi, Anders C. Wulff, Mohammad A. Vesaghi, Jean-Claude Grivel and Mehdi Fardmanesh *Senior Member, IEEE,*

***Abstract*—The effect on the thermal parameters of superconducting transition edge bolometers produced on a single crystalline $SrTiO_3$ (STO) substrate with and without a CeO_2 buffer layer was investigated. Metal organic deposition was used to deposit the 20 nm CeO_2 buffer layer, while RF magnetron sputtering was applied to fabricate 150 nm thick superconducting $YBa_2Cu_3O_{7-\delta}$ (YBCO) thin film. The critical transition temperature for both of the YBCO films was 90 K and the transition width was ∼1.9 K. The bolometers fabricated from these samples were characterized with respect to the voltage phase and amplitude responses, and the results were compared to that of simulations conducted by applying a one-dimensional thermophysical model. It was observed that adding the buffer layer to the structure of the bolometer results in an increased response at higher modulation frequencies. Results from simulations made by fitting the thermal parameters in the model with and without an additional CeO_2 layer were found to be in agreement with the experimental observations.**

***Index Terms*—Transition edge bolometer, Responsivity, YBCO, CeO2 buffer layer**

I. Introduction

SUPERCONDUCTING transition-edge bolometers (TEB) are applied in highly sensitive radiation detectors for a wide range of terahertz applications such as biothermal imaging [1] and in space observatories [2]. The operation principle of these sensors is based on electrically biasing the bolometer and controlling the device temperature to be at the middle of the superconducting transition region. These TEBs are characterized by a broadband functionality [3] in contrast to other types of bolometers. At present, TEBs are limited in relation to concurrent detectivity D* (cm·$\sqrt{\text{Hz}}$/W) and the response time τ (s). However, recent work [4]–[7] has demonstrated that both the detectivity and response time of TEBs may potentially surpass the levels of other radiation detectors. The main effective method for increasing the detectivity in high performance TEBs is optimization of the thermal parameters of the detector [8]–[13] to increase the responsivity r_v (V/W), by which the detectivity is linearly scales. The voltage responsivity of a bolometer is defined as the change in the device voltage per watt of adsorbed radiation power. According to the thermophysical model for TEB detectors [8], the responsivity is defined as:

$$r_\nu = \frac{V}{P} = \frac{\eta I(dR/dT)}{G(1+i\omega_s\tau)} \tag{1}$$

Where I (A) is the bias current, $\frac{dR}{dT}$ (Ω/K) is the temperature variation of the device electrical resistance, G (W/cm·K) is the thermal conductivity of the device, $\tau = \frac{C}{G}$ (s) is the response time of the sensor and ω_s (^{o}) is the angular modulation frequency of the radiation source. Accordingly, thermal parameters affect the magnitude of the response so that a decrease of the thermal conductivity of the whole structure results in higher responsivity. Lowering the thermal capacity of the device, C, results in both a lower response time and a higher responsivity. Therefore, in order to have a highly responsive and high rate detector, the thermal conductivity and the thermal capacity should be as low as possible.

In this work, we evaluate the effect on the voltage response when changing the thermal parameters by adding a CeO_2 buffer layer on a single crystalline $SrTiO_3$ (STO) substrate, on which a YBCO film is deposited and subsequently patterned to form a TEB. These results are compared with both the phase and amplitude response data obtained using a simulated system considering a one-dimensional thermophysical model (see [8]).

II. Experimental

A. Device Preparation

An epitaxial CeO_2 buffer layer was grown on a STO single crystalline substrate using metal organic deposition (see [14] for details). 150 nm thick YBCO thin films were grown on the STO substrates, with and without the CeO_2 layer, by off-axis RF magnetron sputtering system. These YBCO thin films were patterned using standard photolithographic techniques [15] with an accuracy of about 0.6μm, to form a meander-line pattern with 55 μm linewidth providing an active area of 1.44 mm^2 for the device. Considering these dimensions for the pattern, a room temperature resistance of∼ 6.5 $K\Omega$, the critical transition temperature ($T_{C_{onset}}$) of 90 K with R_{onset} around $2.2K\Omega$ and a transition width of ∼1.9 K were obtained for the deposited film. Electrical contacts were produced by mechanically pressing indium spheres onto the patterned film contacts.

Automatically generated dates of receipt and acceptance will be placed here; authors do not produce these dates.

R. Mohajeri, R. Nazifi and M. Fardmanesh are with the Department of Electrical Engineering, Sharif University of Technology, Tehran, Iran. M. Vesaghi is with the Physics Department, Sharif University of Technology, Tehran, Iran.

A. C. Wulff and J-C. Grivel are with the Department of Energy Conversion and Storage, Technical University of Denmark, 4000 Roskilde, Denmark.

This article has been accepted for publication in a future issue of this journal, but has not been fully edited. Content may change prior to final publication. Citation information: DOI 10.1109/TASC.2016.2535144, IEEE Transactions on Applied Superconductivity

B. Measurement Method

A solid state laser diode with a peak wavelength equal to 635 nm, an intensity of $\sim$ 1mW/cm^2 was used as the radiation source, modulated by using an RF pulse generator. Then the optical voltage response of the fabricated bolometer was measured in a DC-current biased mode using four probe configuration technique. The voltage response was amplified by a voltage pre-amplifier (SR560) followed by a lock-in amplifier (SR830), operated at the modulation frequency ω_s for low-noise measurement. The measurement bandwidth was limited by the frequency range of the above-mentioned lock-in amplifier, which is in the range of 1 mHz-102 KHz.

C. Thermophysical Modeling

In order to analyze the effect of the buffer layer on r_v, we used a one-dimensional thermophysical model [8], as well as its closed form solution, to simulate the device response as a function of frequency. Since the thickness values of both the buffer layer and the superconducting film are small compared with the value of the substrate, the former layers (including boundary effects) are considered as a lumped element in the model. The equivalent thermophysical diagram of the device is shown in Fig.1. Considering the buffer layer effect on the

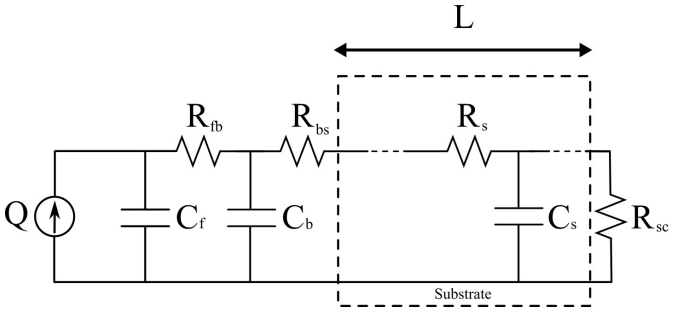

FIG. 1: Equivalent thermophysical model of the layers. Indices relate to sc:substrate-cold head, s:substrate, b:buffer, bs: buffer-substrate, fb: film-buffer, f:film, L: substrate thickness, Q: radiation power, R: thermal resistance, C: thermal capacitance

thermal behavior of the device and according to the equivalent thermophysical model [8], ΔT, which is the temperature variation on the film surface due to Q, the heat flux as a result of radiation absorption at the film surface, is as follows:

$$\Delta T = Q\frac{Z_b + R_{fb}}{1 + i\omega Z_b C_f + i\omega R_{fb} C_f} \tag{2}$$

where, R_{fb} and C_f are the YBCO film-buffer thermal boundary resistance and the heat capacity due to the superconducting film and the interface effects, respectively. Z_b is the equivalent thermal impedance at the buffer layer surface, which is:

$$Z_b = \frac{Z_s + R_{bs}}{1 + i\omega Z_s C_b + i\omega R_{bs} C_b} \tag{3}$$

in which R_{bs} and C_b are the thermal characteristics of the buffer layer as well as the interface effects and Z_s is the equivalent thermal impedance at the substrate surface. According to [8]

$$Z_s = \frac{exp(\gamma L) + \Gamma Exp(-\gamma L)}{exp(\gamma L) - \Gamma Exp(-\gamma L)}\left(\frac{1}{i\omega c_s \kappa_s}\right) \tag{4}$$

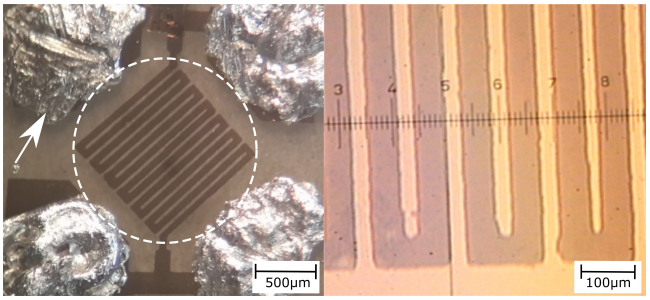

FIG. 2: (Left) the patterned bolometer with the arrow pointing to the indium contacts and the dashed circle around the main bolometer pattern; (right) the exact size of the meander-line width

where γ is the characteristic thermal impedance of the substrate material defined as:

$$\gamma = \frac{1+i}{2^{\frac{1}{2}}}\left(\frac{\omega c_s}{\kappa_s}\right)^{\frac{1}{2}} \tag{5}$$

$$\Gamma = \frac{R_{sc} - \left(\frac{1}{i\omega c_s \kappa_s}\right)}{R_{sc} + \left(\frac{1}{i\omega c_s \kappa_s}\right)} \tag{6}$$

where ω is the angular modulation frequency and κ_s and c_s are distributed heat parameters of the substrate materials and R_{sc} is the thermal boundary resistance between the substrate and the cold head as a constant low-temperature reservoir.

III. Results and Discussion

An optical image of the fabricated TEB showing the meander-line pattern (white dashed circle) and contact points indicated by the white arrow is presented in Fig. 2(left). As shown in the optical image (see Fig. 2(right)), the meander-line pattern is made of about 55 μm wide YBCO tracks. Using these dimensions and the material parameters of STO substrate (C_s and K_s) [8], the thermal parameters presented in Table I were obtained by curve fitting of the experimental data using the closed form solution for the thermophysical model. Thus, analysis of the device was conducted to simulate the characteristic thermal parameters for the device with and without the CeO_2 buffer layer.

TABLE I: Thermal parameters of the samples obtained using the thermophysical model for the samples with and without a buffer layer.

Thermal Parameter	With buffer layer	Without buffer layer
$C_s(\frac{J}{Kcm^3})$[8]	0.43	0.43
$K_s(\frac{W}{Kcm})$[8]	0.05	0.05
$R_{sc}(\frac{Kcm^2}{W})$[8]	5.8	6
$R_{bs}(\frac{mKcm^2}{W})$	46	–
$R_{fb}(\frac{mKcm^2}{W})$	69	–
$R_{fs}(\frac{mKcm^2}{W})$	–	46.6
$C_b(\frac{mJ}{Kcm^2})$	7.9	–
$C_f(\frac{mJ}{Kcm^2})$	0.58	5.1

According to the results from Table I, the thermal resistance between the superconducting film and the substrate is increased due to two thermal boundary effects (R_{bs}, R_{fb}) for the sample with buffer layer compared to the thermal boundary resistance (R_{fs}) for the non-buffered sample. It has previously

This article has been accepted for publication in a future issue of this journal, but has not been fully edited. Content may change prior to final publication. Citation information: DOI 10.1109/TASC.2016.2535144, IEEE Transactions on Applied Superconductivity

been suggested that the heat capacity in high frequencies may be affected by the interface effects [16] reported as C_f and C_b in Table I. Plotting the phase and amplitude of the voltage response using the values from the simulation was done by normalizing equation 2 in combination with equation 1.

The voltage response of the fabricated bolometer is delayed with respect to the adsorbed radiation power due to the thermal parameters of the device, indicated by the phase of the response. Considering the penetration depth of the incoming light, the effect of the thermal capacity of STO substrate and the thermal conductivity of the substrate-cold head boundary are dominant at lower frequencies (up to 10^2 Hz). At midrange frequencies, the thermal properties of the substrate results in a plateau in the phase of the response, while at higher frequencies, the film-substrate thermal boundary properties affect the voltage response behavior [8]. Fig.3 shows the phase of the response for both the measurement and the simulation results for the sample without a buffer layer. This curve is characterized by some low level noise and a few minor kinks. Only a small discrepancy is evident between the experimental and simulated curves which indicates that the simulated curve is in agreement with the measured curve.

To calculate the frequency response of the sample without the buffer layer, Z_b and R_{fb} in 2 were replaced respectively by Z_s and R_{fs} , which effectively results in bypassing the effect of the buffer layer in the above equations. At high frequencies, the thermal behavior of the film-substrate boundary is dominating as confirmed by both the experimental and simulated curves. It is suggested that differences in electronic and vibrational properties in the different materials may scatter the energy at the interface [17] and affect the response as a result of changed heat transfer through the boundary.

The phase response (experimental and simulated) as a function of frequency for the sample with an added CeO_2 buffer layer is presented in Fig. 4. The results for this sample were also characterized by investigating the phase response as a function of frequency. However, this sample demonstrates a plateau in the phase response between 10^2-10^3 followed by an increase in contrast to the sample without a buffer layer. This in-phase behavior at higher frequencies (10^3-10^5) is likely a result of a decreasing interface thermal conductivity due to added buffer layer. Again, only a small discrepancy is observed between the experimental and simulated curves.

Comparing the phase response results for the samples with and without a buffer layer (see Fig. 4 and Fig.3) it is evident that at lower modulation frequencies, the phase responses are similar. While, due to the small thickness of the YBCO film, the effect of the buffer layer becomes significantly more apparent at high–end modulation frequencies as also confirmed by the results from the simulation.

Fig. 5 shows the measured results of the amplitude responses (normalized voltage response) for the samples with and without the added buffer layer. The cut-off frequency of the device is ∼8 Hz, depending on the magnitude of the substrate-cold head thermal conductivity and the thermal capacity of the substrate, which is the same for both samples. Therefore, by decreasing these two parameters, the higher cut-off frequency is expected. Both responses show a decrease

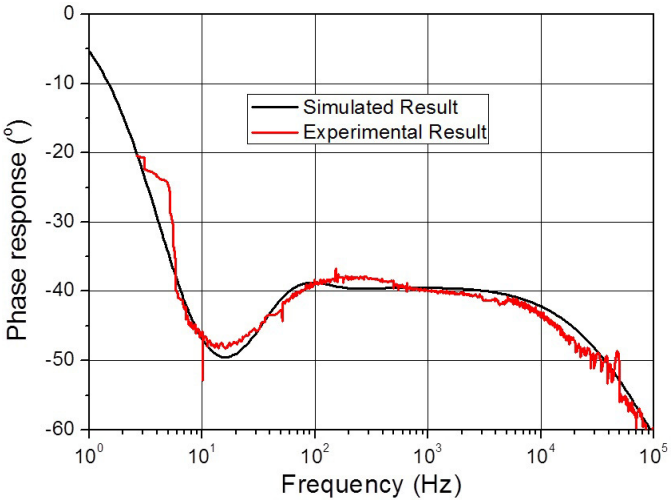

FIG. 3: Simulation and experimental results of the phase response for the sample without a buffer layer.

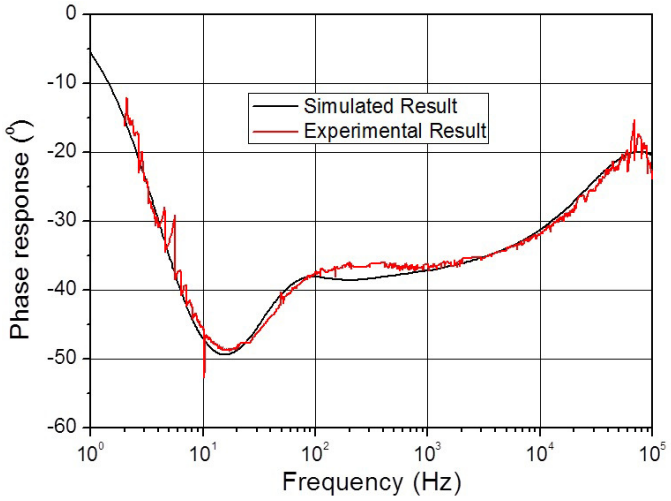

FIG. 4: Simulation and experimental results of the phase response for the sample with a buffer layer.

with increasing frequency and with a very similar behavior up to $\sim 2 \cdot 10^4$ Hz which is attributed to the dominating STO substrate and the substrate-cold head interface thermal parameters. It should be noticed that according to the simulation results (see Fig. 6) the thermal behavior of the sample with an added buffer layer would result in a significantly higher amplitude response (by a factor of ∼6) compared to the sample without a buffer layer at a modulation frequency of about 1 MHz. The observed response is attributed to the increased thermal boundary resistance due to the added buffer layer in higher frequencies. Such a behavior is supported by the high similarity between the curves presented for the measured and simulated data, experimentally verified until frequencies around 10^5 Hz due to the limit of the current setup. It is apparent that further works should focus on the investigations of the variation of the added buffer layer, the effect of adding more buffer layers and experimental characterization at elevated modulation frequencies.

This article has been accepted for publication in a future issue of this journal, but has not been fully edited. Content may change prior to final publication. Citation information: DOI 10.1109/TASC.2016.2535144, IEEE Transactions on Applied Superconductivity

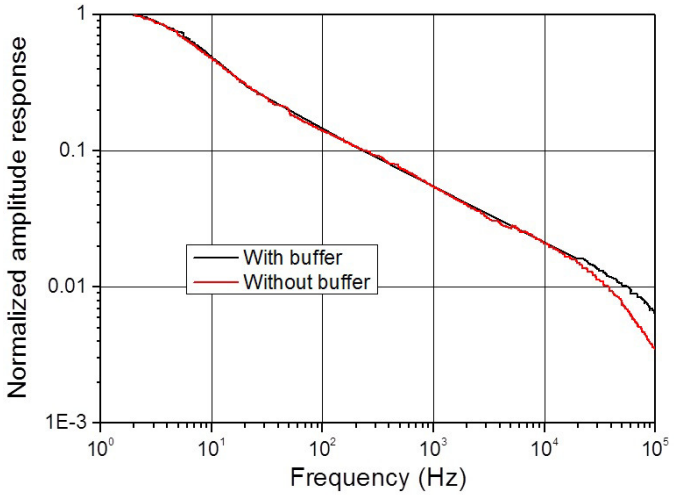

FIG. 5: Amplitude response of the samples with and without a buffer layer. Notice that the scale of the frequency is up to 10^5.

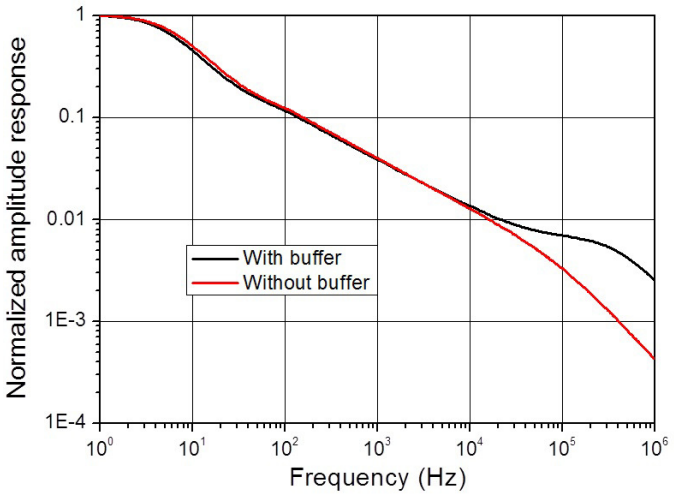

FIG. 6: Simulation results for the amplitude response of samples with and without a buffer layer. Notice that the scale of the frequency is up to 10^6.

IV. Conclusion

Superconducting YBCO-based transition-edge bolometers with and without an added CeO_2 buffer layer on STO substrates were produced and investigated with respect to phase and amplitude response during irradiation with a frequency-modulated light source. These superconducting samples were characterized by a critical transition temperature of 90 K and a transition width of $\sim$1.9 K. A one-dimensional thermophysical model was applied to simulate thermal parameters of the bolometers and response curves based on these data were compared with measured results. Both the measured and simulated data provided evidence that adding buffer layer leads to an increased in-phase response at higher frequencies which is an indication of the increased surface thermal boundary resistance. Therefore, significant increase in the amplitude response was observed at frequencies between 10^4-10^6 Hz for the sample with a buffer layer compared to the values for the sample without buffer layer. The increased voltage response of the bolometer at high modulation frequencies provides the use of this kind of sensors for the application of arrayed bolometers with high scanning speed.

Acknowledgment

The authors would like to thank M. Esmaeili (Department of Electrical and Computer Engineering, Sharif University of Technology, Tehran, Iran) for her assistance for the response-measurement setup.

References

[1] A. Ahmed, R. Tait, T. B. Oogarah, H. Liu, M. W. Denhoff, G. Sproule, and M. Graham, "A surface micromachined amorphous gexsi1-xoy bolometer for thermal imaging applications," in *Photonics North*. International Society for Optics and Photonics, 2004, pp. 298–308.

[2] V. Revéret and L. Rodriguez, "Progress on silicon bolometers for (sub)-millimeter astronomy: from artémis to future b-mode detection space missions."

[3] P. Richards, "Bolometers for infrared and millimeter waves," *Journal of Applied Physics*, vol. 76, no. 1, pp. 1–24, 1994.

[4] A. Moftakharzadeh, A. Kokabi, M. Banzet, J. Schubert, and M. Fardmanesh, "Detectivity analysis and optimization of large-area freestanding-type hts bolometers," *Applied Superconductivity, IEEE Transactions on*, vol. 22, no. 2, pp. 2 100 107–2 100 107, 2012.

[5] A. Moftakharzadeh, A. Kokabi, A. Bozbey, T. Ghods-Elahi, M. Vesaghi, S. Khorasani, M. Banzet, J. Schubert, and M. Fardmanesh, "Detectivity of ybco transition edge bolometer: modulation frequency, bias current and absorber effects," in *Journal of Physics: Conference Series*, vol. 97, no. 1. IOP Publishing, 2008, p. 012009.

[6] M. Fardmanesh, K. J. Scoles, and A. Rothwarf, "Control of the responsivity and the detectivity of superconductive edge-transition ybco bolometers through substrate properties," *Applied optics*, vol. 38, no. 22, pp. 4735–4742, 1999.

[7] M. Hosseini, A. Moftakharzadeh, A. Kokabi, M. A. Vesaghi, H. Kinder, and M. Fardmanesh, "Characterization of a transition-edge bolometer made of ybco thin films prepared by nonfluorine metal–organic deposition," *Applied Superconductivity, IEEE Transactions on*, vol. 21, no. 6, pp. 3587–3591, 2011.

[8] M. Fardmanesh, "Analytic thermal modeling for dc-to-midrange modulation frequency responses of thin-film high-tc superconductive edge-transition bolometers," *Applied optics*, vol. 40, no. 7, pp. 1080–1088, 2001.

[9] P. Neuzil and T. Mei, "Evaluation of thermal parameters of bolometer devices," *Applied physics letters*, vol. 80, no. 10, pp. 1838–1840, 2002.

[10] A. Bozbey, M. Fardmanesh, J. Schubert, and M. Banzet, "Analytical modelling of the interpixel thermal crosstalk in superconducting edge-transition bolometer arrays," *Superconductor science and technology*, vol. 19, no. 6, p. 606, 2006.

[11] G. Hyseni, N. Caka, and K. Hyseni, "Infrared thermal detectors parameters: semiconductor bolometers versus pyroelectrics," *WSEAS Transactions on circuits and systems*, vol. 9, no. 4, pp. 238–247, 2010.

[12] M. Fardmanesh and İ. N. Askerzade, "Temperature dependence of the phase of the response of ybco edge-transition bolometers: effects of superconductivity transition and thermal parameters," *Superconductor Science and Technology*, vol. 16, no. 1, p. 28, 2003.

[13] S.-F. Lee, J. M. Gildemeister, W. Holmes, A. T. Lee, and P. L. Richards, "Voltage-biased superconducting transition-edge bolometer with strong electrothermal feedback operated at 370 mk," *Applied Optics*, vol. 37, no. 16, pp. 3391–3397, 1998.

[14] M. Hosseini, F. F. Abari, M. Vesaghi, and M. Fardmanesh, "Mod growth of epitaxial cerium oxide buffer layer on lao substrates for fabrication of c-axis oriented ybco," *Micro & Nano Letters*, vol. 7, no. 10, pp. 1008–1010, 2012.

[15] M. Fardmanesh, A. Rothwarf, and K. J. Scoles, "Low and midrange modulation frequency response for ybco infrared detectors: interface effects on the amplitude and phase," *Applied Superconductivity, IEEE Transactions on*, vol. 5, no. 1, pp. 7–13, 1995.

[16] J. Ettrich, *Fluid flow and heat transfer in cellular solids*. KIT Scientific Publishing, 2014, vol. 39.

[17] B. Persson, A. Volokitin, and H. Ueba, "Phononic heat transfer across an interface: thermal boundary resistance," *Journal of Physics: Condensed Matter*, vol. 23, no. 4, p. 045009, 2011.